5

Quinone Binding Sites in Reaction Centers from Photosynthetic Bacteria

M. Y. OKAMURA
R. J. DEBUS
D. KLEINFELD
G. FEHER

INTRODUCTION

Quinones have long been known to be involved in photosynthetic electron-transfer reactions (*1*). More recently, quinones were found to form an integral part of the reaction center (RC) of photosynthetic bacteria. The reaction center functions as an energy transducer, converting electromagnetic energy (the absorbed photon) into chemical free energy (the production of a charged donor–acceptor pair). The reaction center protein isolated from bacterial membranes with detergent consists of three subunits (L, M, H) with molecular weights (determined by SDS gel electrophoresis) of 21, 24, and 28 kdalton. It contains four bacteriochlorophylls, two bacteriopheophytins, one Fe^{2+}, and two quinones. For recent reviews on reaction centers, see Loach (*2*), Feher and Okamura (*3*), Dutton *et al.* (*4*), and Okamura *et al.* (*5*). For recent reviews on the role of quinones in reaction centers, see Parson (*6*), Bolton (*7*), and Wraight (*8*).

The primary photochemistry leading to charge separation occurs in several steps, shown schematically in Fig. 1 (*9*, 10). The process begins with absorption of a photon to form the excited state of a tetrapyrrole-pigment complex in which electron transfer occurs from a donor species,

Function of Quinones in Energy Conserving Systems

ISBN 0-12-701280-X

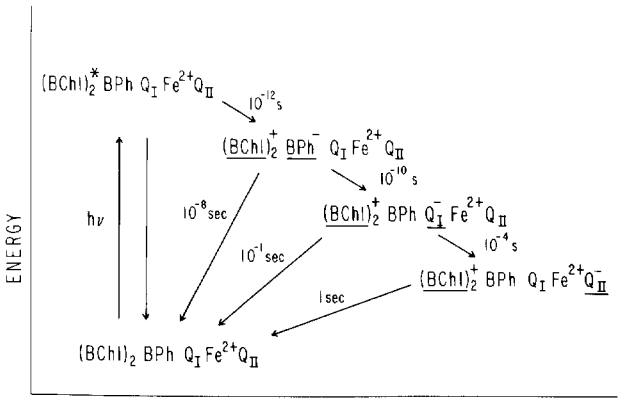

Fig. 1. Schematic representation of the electron-transfer reactions in reaction centers from photosynthetic bacteria. After photon absorption, the electron transfers through a series of reactants that are stabilized against charge recombination for progressively longer periods of time. Charged donor–acceptor species are underlined. Transfer times are given for room temperature and are rounded to the nearest power of 10.

identified to be a bacteriochlorophyll dimer $(BChl)_2$, to an acceptor species, thought to be a bacteriopheophytin molecule (BPh). At this stage, if no other acceptor species is present, decay to the ground state occurs in $\sim 10^{-8}$ sec leading to a loss of photochemical energy. To prevent this loss, another species must accept the electron in a time of less than 10^{-8} sec. The two quinones, Q_I and Q_{II}, perform this task in the bacterial reaction center. The primary quinone, Q_I, reacts with the reduced (BPh) in 10^{-10} sec. Subsequent electron transfer to the second quinone, Q_{II} occurs in 10^{-4} sec. The charge recombinations of $(BChl)_2^+$ with Q_I^- and Q_{II}^- are many orders of magnitude longer, i.e., 10^{-1} sec and 1 sec, respectively.

In reaction centers from *Rhodopseudomonas sphaeroides* R-26, both Q_I and Q_{II} are ubiquinone (UQ-); in *Chromatium vinosum*, Q_I is menaquinone and Q_{II} is UQ-50. In *Rps. sphaderoides*, both Q_I and Q_{II} are magnetically coupled to the Fe^{2+} in what has been called the ferroquinone complex. Under physiological conditions, Q_I accepts only one electron while Q_{II} can accept two electrons. The reactions of Q_I and Q_{II} have been investigated in detail and are discussed elsewhere in this volume.

One important approach in the investigation of quinones in reaction centers was based on the ability to extract them from reaction centers and subsequently reconstitute the reaction centers with the native quinone or a variety of other quinones. The procedure to remove quinones consists either of organic solvent extraction (*11*) or of a gentler method involving incubation with a high concentration of detergent in the presence of the electron-transfer inhibitor, orthophenanthroline (*12*). We shall review

some of the properties of quinones bound to reaction centers isolated from *Rps. sphaeroides* R-26 and discuss some of the results from our laboratory. Many of the results are based on removal and reconstitution studies. The main questions we have posed are: Where on the reaction centers are the quinones bound? What is the nature of the quinone binding sites? How do the quinones interact with their neighbors, particularly (BPh) and Fe^{2+}? Some of the results discussed here have been presented previously, and others are preliminary in nature.

EXPERIMENTAL RESULTS

Quinone Assays by Photochemical Activity

The most straightforward but tedious procedure to determine the number of quinones bound to reaction centers is by chemical analysis (*12*). Several faster and simpler spectrophotometric procedures have been developed and are now routinely used.

PHOTOACTIVITY AT CRYOGENIC TEMPERATURES At temperatures less than 80 °K, electron transfer to Q_{II} is not observed to occur. Consequently, photochemical activity of reaction centers at these temperatures can be used to assay for electron transfer to Q_I. Most conveniently, the extent of bleaching of the spectral band at 890 nm, associated with the oxidation of $(BChl)_2$, can be used to monitor the electron transfer.

PHOTOACTIVITY AND CHARGE RECOMBINATION KINETICS AT ROOM TEMPERATURE Another quinone assay utilizes the flash-induced bleaching and recovery of $(BChl)_2$ monitored at 865 nm at room temperature (Fig. 2A). The amplitude of the bleaching is proportional to the amount of Q_I present (Fig. 2B). At room temperature, electron transfer from Q_I to Q_{II} occurs and forms the basis of an assay sensitive to the presence of Q_{II}. It utilizes the difference in charge recombination times between $(BChl)_2^+$ and Q_I^- ($\sim$0.1 sec) and between $(BChl)_2^+$ and Q_{II}^- ($\sim$1 sec; *13*, *14*). By decomposing the charge recombination kinetics into fast and slow phases, the amounts of photochemically active Q_I and Q_{II} can be determined (Fig. 2C). However, only 80%, rather than 100%, slow phase was observed in reaction centers having an average of 2.0 quinones per reaction center, determined by chemical analysis. In these reaction centers, $\sim$0.2 quinones were not

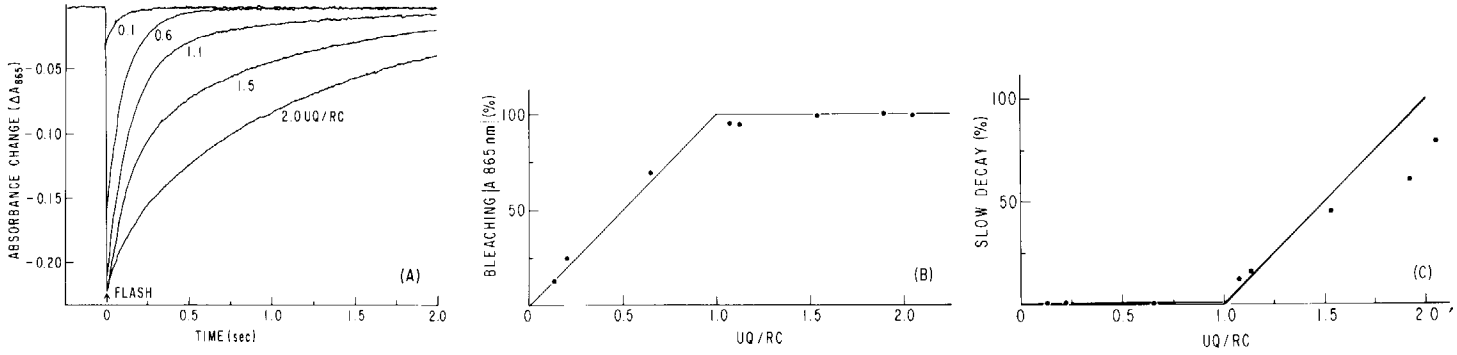

Fig. 2. Room temperature kinetic assay. (A) Formation and decay of $(BChl)_2^+$, monitored at 865 nm, in reaction centers containing different mole fractions of UQ-50. The reaction centers (2.0 μM in 0.025% LDAO, 10 mM Tris-Cl, pH = 8, at T = 23 °C) were given a 0.3 μsec laser flash (λ = 584 nm). The quinone content was determined chemically. (B) Amplitude of bleaching (expressed as percent of the maximum) as a function of mole fraction of bound quinones. The solid curve is the expected result if one quinone binds much more strongly than the second. (C) Percent slow phase as a function of mole fraction quinone. The slow component ($\tau_D \simeq 1.2$ sec) was obtained by plotting the logarithm of the amplitude of the curves in (A).

reduced by Q_I^- after a single flash. These quinones, however, appear to be reduced under continuous illumination of the reaction centers (see Fig. 3). Thus, they may be bound to an altered Q_{II} binding site or to another site nearby.

PHOTOOXIDATION OF CYTOCHROME c An alternate assay, sensitive to the presence of both quinones, utilizes the rapid oxidation of cytochrome *c* by reaction centers under continuous illumination (*13*, *15*, *16*). The number of cytochromes oxidized during the rapid phase of the absorption change at 550 nm equals the number of electrons used in the reduction of the bound quinones. The rise time of the fast phase of cy-

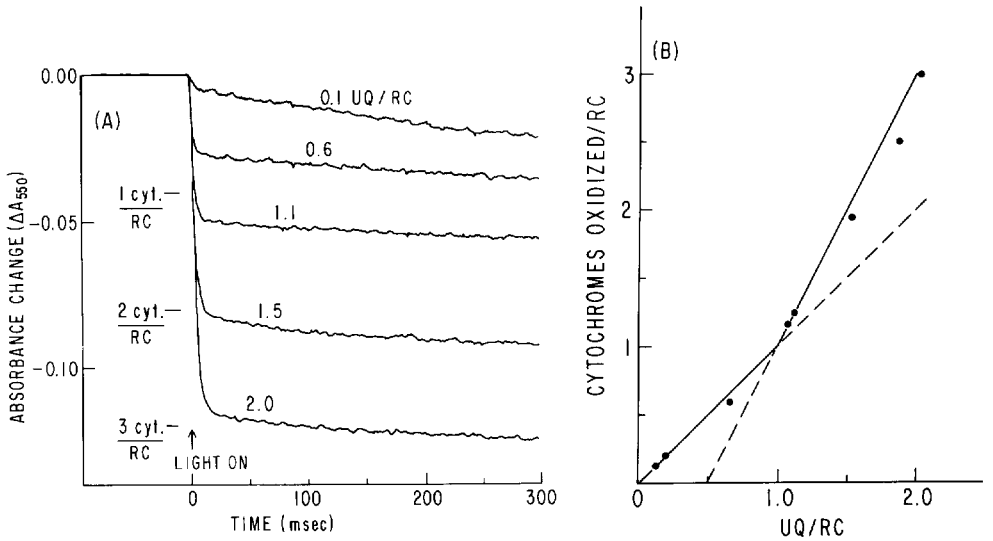

Fig. 3. Cytochrome photooxidation assay. (A) Optical absorption change at 550 nm versus time caused by cytochrome *c* oxidation by reaction centers containing different mole fractions of UQ-50. Reaction centers (2.0 μM in 0.025% LDAO, 10 mM Tris-Cl, pH 8, at T = 23 °C) with 20 μM reduced cytochrome *c* (horse heart) were illuminated with near IR light (Tungsten lamp filtered by 2 cm of H_2O and a Corning CS 2-64 filter giving $I \simeq 800$ mW/cm^2) in an optical kinetics spectrometer (*51*). The number of cytochrome *c* oxidized per reaction center was determined from the relation

$$\frac{\text{cyt. } c \text{ oxidized}}{\text{RC}} = 14.4\,(\Delta A_{550\text{ nm}}/A_{802\text{ nm}})$$

The UQ-50 content was determined chemically [Okamura, *et al.* (12)]. It was assumed that at the low detergent concentration used, all quinones are bound to the reaction center. (B) The plot of cytochromes oxidized per RC versus UQ per RC. The solid line is the curve expected if the primary quinone accepts one electron and the secondary quinone accepts two electrons, and the binding of Q_I is much stronger than Q_{II}.

tochrome oxidation is limited by the light intensity. The slower phase (see Fig. 3A) is caused by electrons escaping from reduced acceptors. Since Q_I normally accepts only one electron while Q_{II} accepts two electrons, we expect that reaction centers with one and two bound quinones can oxidize one and three cytochromes, respectively. This was observed experimentally for reaction centers containing a variable number of quinones (see Fig. 3B).

Quinone Structure–Function Relationships

Using the assay procedures described, we investigated the effect of the quinone structure on photochemical activity. Quinones solubilized in ethanol or the detergent lauryldimethylamine oxide (LDAO) were added to reaction centers depleted of quinone. The binding of quinone to the Q_I site was determined from room temperature photoactivity measurements. Estimates of the dissociation constants, $C_{1/2}$, were obtained from the amount of quinone required to produce half the maximum photoactivity. In view of the low solubility of many quinones, it is not clear whether an equilibrium binding constant was measured. Consequently, the data for $C_{1/2}$ should be taken as only qualitatively correct. The charge recombination times, τ_D, were determined from the decay of the optical changes at 865 nm. The results of a survey of various quinones are shown in Table I.

Binding to the *primary* site occurs with high affinity, especially for quinones with side chains (Table I). Generally, addition of a stoichiometric amount of these quinones ($\sim 1\ \mu M$) will result in a significant degree of reconstitution. Reaction center charge recombination times from Q_I vary greatly with the structure of the quinone (Table I). All quinones studied, except for anthraquinone, have a recombination time that increases with increasing temperature. In anthraquinone, the opposite temperature dependence is found, as expected for a thermally activated process. A detailed investigation of the temperature dependence of this reaction is currently underway and may give some insight into the mechanism of electron transfer.

The binding of quinone to the secondary site is weaker than to the primary site. In addition, the requirements for activity appear to be more specific. The observation of biphasic charge recombination kinetics after a saturating light pulse was observed only when ubiquinones with isoprenoid side chains were used to reconstitute reaction centers. An interesting observation is that the ubiquinone analog UQ-0-decyl does not induce slow phase recombination kinetics. The only difference

TABLE I

Binding Constants and Charge Recombination Times for Reaction Centers Reconstituted with Different Quinones[A]

Quinone	Primary site		Secondary site	
	$C_{1/2}$[B] (μM)	τ_D[C] (sec)	$C_{1/2}$[D] (μM)	τ_D[E] (sec)
UQ-50[F]	<1	0.12	~5	1.2
UQ-10	<1	0.17	~5	1.8
UQ-0-decyl	<1	0.24	>50	—
UQ-0	~10	0.18	>50	—
Vitamin K_1	<1	0.078	>50	—
Menadione	<1	0.16	>50	—
Duroquinone	<1	0.55	>50	—
Anthraquinone[F]	~10	0.01	>50	—

[A] Samples in 10 mM Tris-Cl, 0.025% to 0.2% LDAO, 1 mM EDTA, pH 8.0 $T \simeq 23$ °C.
[B] Concentration of quinone required to produce half-maximum amount of fast phase.
[C] Time required for the amplitude of the fast phase of the 865 nm absorbance change to decay to 1/e of its maximum value.
[D] Concentration of quinone required to produce half-maximum amount of slow phase.
[E] Time required for the amplitude of the slow phase of the 865 nm absorbance change to decay to 1/e of its maximum value.
[F] Quinone added in LDAO solution.

between this quinone and UQ-10 is that it contains a ten-carbon straight chain instead of a ten-carbon isoprenoid chain. Either UQ-0 decyl does not bind to the Q_{II} site or it binds and is not active. To distinguish between these two possibilities, UQ-0-decyl was tested for its ability to compete with UQ-50 for the Q_{II} site. The results (Fig. 4) show that UQ-0-decyl, when added to reaction centers containing UQ-50 in the Q_{II} site, causes a decrease in the amount of slow phase kinetics. This suggests that UQ-0-decyl binds at the Q_{II} site. The lack of photochemical activity with UQ-0-decyl could arise from either kinetic constraints (i.e., a significant increase in the electron-transfer time from Q_I to Q_{II}) or thermodynamic constraints (i.e., stabilization of $Q_I^- Q_{II}$ relative to $Q_I Q_{II}^-$). These results indicate the highly specific requirements imposed on the structure of Q_{II}.

Location of the Quinone Binding Sites

The location of the Q_I binding site has been determined by Marinetti *et al.* (*17*) using the technique of photoaffinity labeling. The photoaffinity label [H^3]2-azido-anthraquinone was added to quinone-depleted

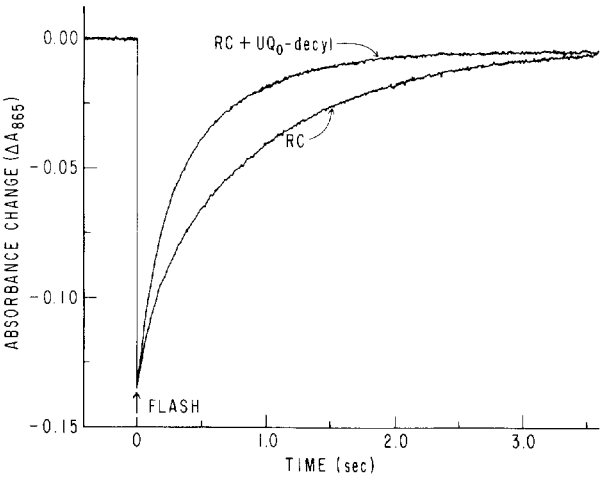

Fig. 4. The effect of UQ-0-decyl on the slow phase of the recombination kinetics. The lower curve (RC) was obtained as in Fig. 2A for reaction centers (1.1 μM) containing ~1.8 UQ-50. The upper curve shows the effect of adding UQ-0-decyl (17 μM) to these reaction centers. The increase in the decay rate indicates an inhibition of electron transfer from Q_I to Q_{II} believed to be caused by the successful competition of the photochemically inactive UQ-0-decyl for the Q_{II} binding site.

reaction centers and found to restore photochemical activity. Excess azido-anthraquinone was added to saturate the primary binding site and excess quinone was washed off by DEAE cellulose chromatography. Since at low detergent concentrations Q_I exchanges only slowly with the external medium, reaction centers containing anthraquinone in the Q_I binding site were obtained. Photolysis of this sample, followed by SDS polyacrylamide gel electrophoresis, showed a specific labeling of the M subunit (see Fig. 5), indicating that Q_I binds on or near M.

Photoaffinity labeling of the Q_{II} binding site has not been accomplished due to the more stringent structural requirements for the secondary quinone. Instead, an immunological approach has been used to locate this site. Antibodies against specific RC subunits were isolated using affinity chromatography (*18*). All of these were shown by radioimmunoassay to bind to reaction centers. These antibodies were tested to see if they could block electron transfer from Q_I to Q_{II} using the kinetic assay as described in the previous section (*19*). In order to prevent precipitation of the RC-antibody complex, Fab fragments made by papain digestion were used. The conditions of the assay (0.1% LDAO, 1 μM UQ-50, 0.2 μM RC) were chosen so that in the absence of antibodies 50% of the reaction centers showed the slow charge recombination kinetics due to

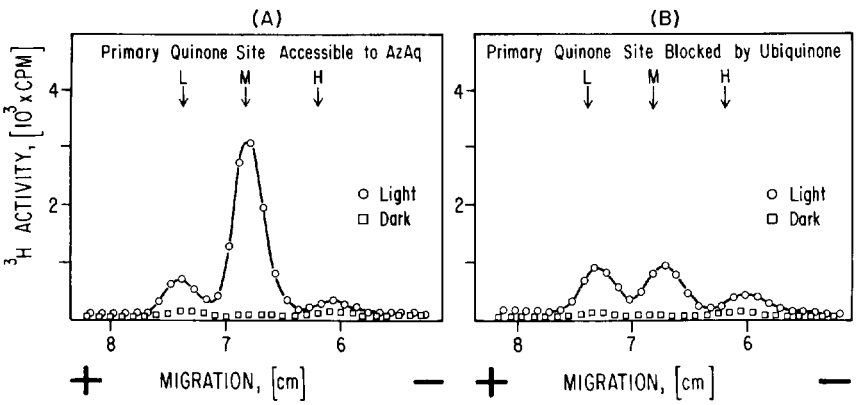

Fig. 5. SDS polyacrylamide gel electrophoretograms of reaction centers reconstituted and labeled with 2-azido[^{3}H]anthraquinone (AzAq). (A) Reaction centers depleted of UQ-50 and reconstituted with azido anthraquinone. (B) Reaction centers with UQ-50 in the Q_I site treated as in A. [From Marinetti *et al.* (*17*), used with permission.]

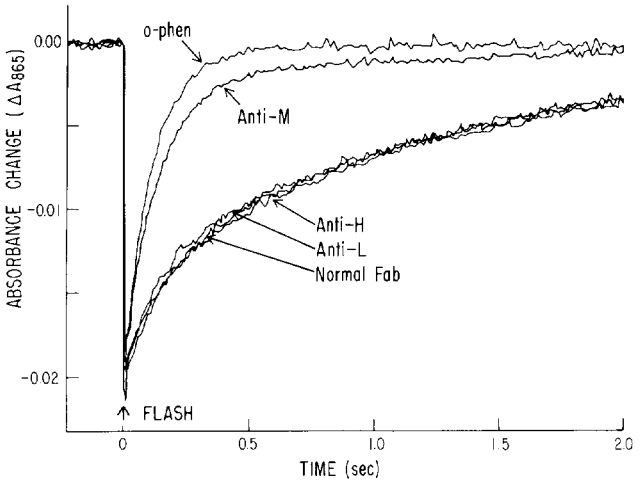

Fig. 6. Antibody inhibition of Q_{II} activity as measured by the kinetics of charge recombination (see Figs. 2A and 4). Fab fragments from affinity purified antibodies (3 μM) were added to reaction centers (0.2 μM) in the presence of 1 μM UQ-50 (0.1% LDAO, 10 mM Tris, 14 μM EDTA, pH 8.0). Fab made from normal antibodies was used as a control. Addition of anti-M Fab resulted in an increase in the charge recombination rate similar to that produced by 5 mM *o*-phenanthroline, a known inhibitor of electron transfer to Q_{II}. The simplest explanation of these results is that anti-M Fab inhibits the binding of Q_{II}.

electron transfer from Q_{II}^- to $(BChl)_2^+$. Addition of antibodies against the M subunit greatly decreased the amount of the slow component (see Fig. 6) while antibodies against the L or H subunits did not. This was true for all Fab preparations from different antisera (five M, three L, and two H antisera were tested). The inhibition of electron transfer occurred whether UQ-10 or UQ-50 was used as the secondary quinone. The simplest interpretation of these results is that binding of anti-M Fab at the Q_{II} site inhibits either binding or activity of the secondary quinone. Thus, both Q_I and Q_{II} appear to be bound on the M subunit. Further experiments are in progress to verify this. Although antibodies to the H subunit had little or no effect on the amplitude of the slow component, one of the two anti-H antisera produced a 20% increase in the rate of the slow phase. This suggests that the environment of Q_{II} is affected by the H subunit.

Further evidence of the possible role of the H subunit is provided by recent experiments involving dissociation and reconstitution of the H subunit. When the H subunit was dissociated from the reaction center, the remaining LM-pigment complex retained the primary photochemical reactants (including Fe^{2+}) and exhibited full photochemical activity (*3*, *20*). Electron transfer from Q_I in LM differs from that in reaction centers as shown by the photooxidation of cytochrome *c* (Fig. 7). Only one cytochrome *c* was rapidly oxidized by LM, even in the presence of excess UQ-50. When the H subunit was reconstituted with LM, the amount of rapidly oxidized cytochrome *c* was increased (*21*). This indicates that either the binding or the activity of Q_{II} is altered when the H subunit is removed.

Interaction of Quinone with Fe^{2+}

EPR The observation of a broad EPR signal (*22–24*) from the reduced primary acceptor (Fig. 8a) and the presence of Fe^{2+} in the reaction center led to the concept of an iron-quinone complex in which the electron is primarily localized on the quinone. The large width of the EPR signal is due to the magnetic interaction between Q_I^- and Fe^{2+}. This assignment is supported by several different observations (*3*) including the important observation of photochemical activity in iron-free reaction centers. In these preparations a new EPR signal (Fig. 8b) was observed (*25*) and identified as arising from a UQ anion radical (*26*). Subsequent work showed a broad EPR signal is also observed when Q_{II} is singly reduced (*27–29*), indicating that a similar magnetic interaction

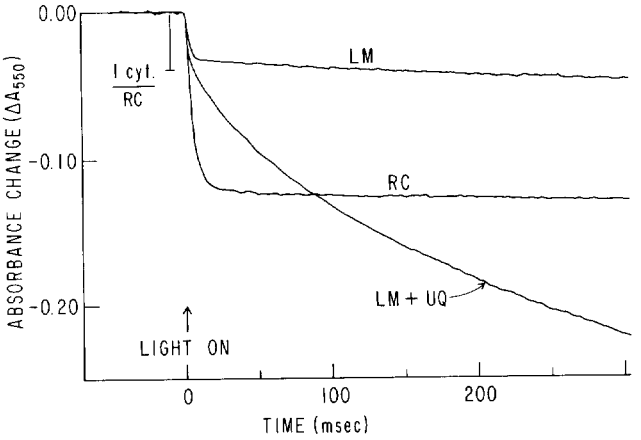

Fig. 7. Cytochrome photooxidation assay of the LM subunit. The LM subunits were prepared as described by Feher and Okamura (*3*). The cytochrome photooxidation assay was performed as in Fig. 2 and shows only one cytochrome *c* per reaction center oxidized during the fast phase (2.0 μM LM, 20 μM cytochrome *c*, 0.18% cholate, 0.2% deoxycholate, 1 mM EDTA, 10 mM Tris-Cl, pH = 8). When excess UQ-50 (30 μM) was added in deoxycholate, still only ~1 cytochrome *c* per reaction center was oxidized in the fast phase, although an increase in the slower rate of cytochrome oxidation was observed. The increase suggests that removal of the H subunit exposes Q_I^- to the exogenous UQ-50 which acts as an electron acceptor. The cytochrome photooxidation kinetics for reaction centers in LDAO is shown for comparison.

exists between Q_{II}^- and Fe^{2+}. A possible role of iron is to facilitate electron transfer from Q_I to Q_{II}, the "Iron-wire Hypothesis" (*12*). Support for this hypothesis has come from the observation by Blankenship and Parson (*14*) that reaction centers depleted of iron cannot transfer electrons from Q_I to Q_{II}. It should be noted that their procedure used to remove Fe^{2+} and our procedure used to dissociate H are very similar. Consequently, the loss of electron transfer from Q_I to Q_{II} which they observed may have been caused by loss of H rather than of Fe^{2+} (*21*).

MAGNETIC SUSCEPTIBILITY From the temperature dependence of the magnetization of reaction centers, the parameters (e.g., *g*-value, crystalline field splittings) characterizing the electronic structure of the paramagnetic Fe^{2+} were deduced (*30*). Since these parameters depend on the nature of the Fe^{2+} ligands, determination in reaction centers containing varying amounts of quinones can be used to determine whether the quinones are coordinated to the Fe^{2+}.

No changes in magnetization were observed between reaction cen-

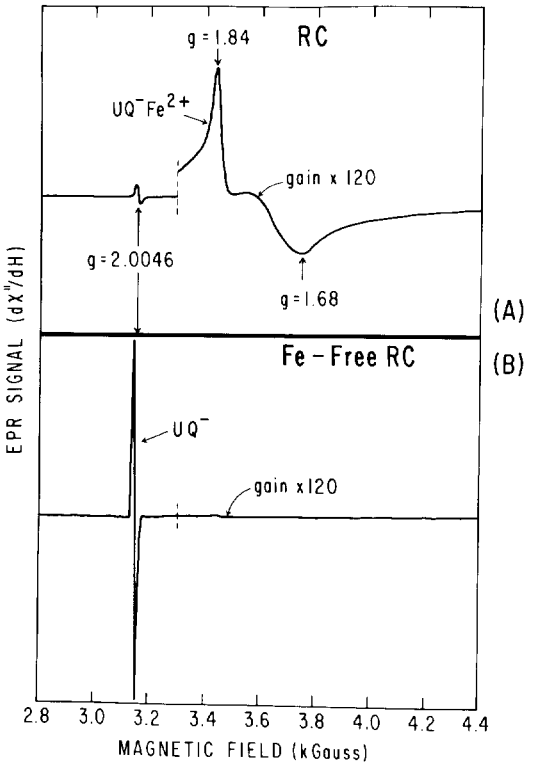

Fig. 8. EPR spectra of the reduced primary quinone in RCs (A) with reaction centers Fe and (B) without Fe. Both samples were reduced with 50 m*M* dithionite, 100 m*M* Tris-Cl, pH = 8, and quickly frozen to cryogenic temperatures. The Fe-free sample was prepared as described by Feher and Okamura (*3*). The spectrometer gain and microwave power were increased above 3.3 kG to observe the broad signal. The *g*-value (2.0046) of the narrow signal was obtained from a slower scan and is identical to that of UQ-50$^-$ (*24*). The broad EPR signal is thought to be due to Q_I^- magnetically coupled to Fe^{2+}; ν = 8.85 GHz, T = 2.1 °K.

ters containing one and two quinones, indicating that Q_{II} is not coordinated to Fe^{2+}. However, changes occurred when Q_I was removed that can be ascribed to either a loss of ligation of Q_I to Fe^{2+} or to a conformational change of the protein. One argument in favor of a conformational change is that EPR data indicate that the interaction of Fe^{2+} with Q_I is approximately the same as with Q_{II}. Since we argued previously that Q_{II} is not a ligand of Fe^{2+}, we infer that neither is Q_I.

From the magnetization measurements of reduced reaction centers (i.e., $Q_I^-Fe^{2+}$), the magnetic exchange interaction, J, between the spin on Q_I^- and the spin on the Fe^{2+} was obtained (*30*). The small value of the

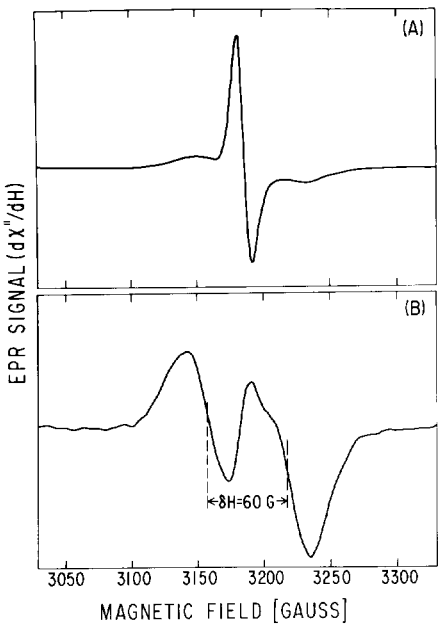

Fig. 9. EPR spectrum of reaction centers reconstituted with menaquinone (vitamin K_1) after rapid photoreduction at low redox potential. (A) At low power, (10^{-6} W, T = 2.1 °K, ν = 8.90 GHz) the narrow singlet signal of reduced (BPh) appears. Additional lines appear on the wings. At high (10^{-2} W, T = 2.1 °K, ν = 8.90 GHz) microwave power (B) the singlet signal is greatly reduced due to microwave saturation and the doublet signal predominates. The doublet signal is believed to be caused by an interaction between the (BPh) radical and the reduced menaquinone-Fe^{2+} complex. [From Okamura *et al.* (*43*), used with permission.]

interaction energy ($|J| < 1$ cm^{-1}) compared with those of other model compounds (*31*, *32*) provides an independent indication that Q_I is not coordinated to Fe^{2+}.

MOSSBAUER SPECTROSCOPY Reaction centers with different numbers of quinones were prepared from bacteria grown on a synthetic medium enriched in Fe^{57}. The two main quantities that are measured by Mossbauer spectroscopy are the isomer shift, δ, and the quadrupole splitting parameter, ΔE_Q. These quantities provide a sensitive measure of the iron environment. The values of δ and ΔE_Q were found to remain essentially unchanged when either one or both quinones were removed (*33*). These results indicate that either the quinones are not ligands of the iron, or that their removal is accompanied by a replacement with a similar ligand.

EXAFS The nature of the ligands around the Fe^{2+} were examined by extended x-ray fine-structure spectroscopy (EXAFS) (*34–36*). In this technique, the x-ray absorption spectrum close to the Fe^{2+} absorption edge (~7.2 keV) is measured. The spectrum shows oscillations caused by the scattering of photoelectrons from neighboring ligands. These oscillations provide a sensitive probe for investigating the number and nature of the ligands around Fe^{2+}. EXAFS spectra, obtained

from reaction centers with one or two quinones showed no difference in number of ligands and average ligand distance from Fe^{2+} (<0.02 Å). In addition, no effect on the EXAFS spectrum was observed when orthophenanthroline was added. These results were interpreted to indicate that neither Q_{II} nor orthophenanthroline coordinates to Fe^{2+}. However, the EXAFS spectrum of reaction centers with no bound quinones showed a significant decrease (~12%) in amplitude. This reduction in amplitude may indicate Q_I coordination to Fe^{2+} or may be explained by a conformational change of the reaction center protein. In view of other experimental evidence, we favor the latter explanation.

Interaction of Quinone and Bacteriopheophytin

The primary quinone accepts an electron from reduced (BPh) in 10^{-10} sec (*37*, *38*). The rapid rate of this reaction implies a strong interaction between these species. The first evidence for an interaction between (BPh) and Q_I came from observation of an electrochromic shift in the optical spectrum of (BPh) when Q_I was reduced (*39–41*). Electrochromic shifts in the spectrum of (BPh) were also seen when Q_{II} was reduced (*41*). Evidence for the interaction between (BPh) and Q_I was first obtained in reaction centers from *C. vinosum*, where a doublet EPR signal was observed after photoreduction of (BPh) at low redox potential (*42*). Under the same conditions a doublet EPR signal was not observed in native reaction centers of *Rps. sphaeroides*. However, a doublet signal appeared (see Fig. 9) when the native Q_I (UQ-50) was replaced by Vitamin K_1, similar to the primary quinone in *C. vinosum* (*43*). The doublet splitting was assigned to an exchange interaction ($|J|$ = 60 G) between $(BPh)^-$ and the MQ^-Fe^{2+} complex. This interaction arises from an overlap of electronic wavefunctions and is directly related to the rate of electron transfer between $(BPh)^-$ and Q_I^- according to a theory of thermally activated electron tunneling (*44*). The exchange interaction can be related to the distance between $(BPh)^-$ and Q_I^-. Using a simple model, this distance was estimated to be 7 to 10 Å (*43*). Other workers (*45*, *46*) have estimated similar distances.

Nature of the Quinone Binding Site

OPTICAL ABSORPTION SPECTROSCOPY One of the simplest probes of the quinone environment in reaction centers is its optical absorption spectrum. In reaction centers, optical difference spectra (reduced minus oxidized) of both Q_I and Q_{II} show an absorption peak near

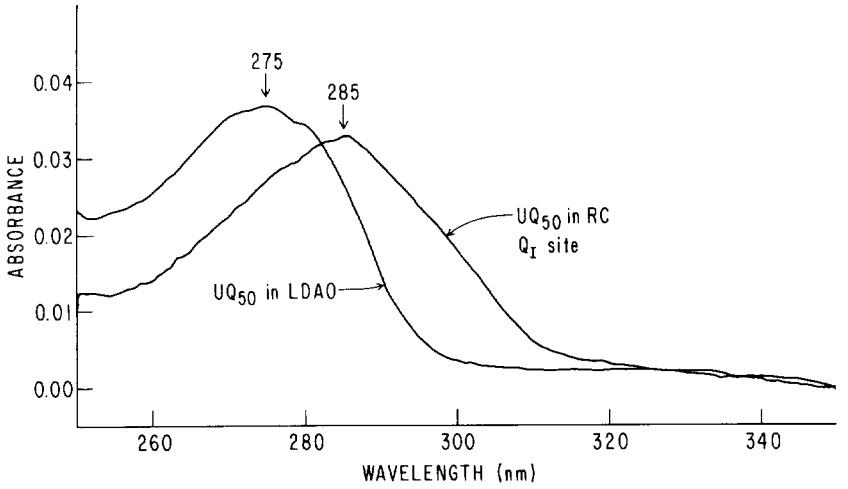

Fig. 10. Optical absorbance changes of UQ-50 in reaction centers and in detergent solution. The optical spectra were obtained with a CARY 14R spectrophotometer. The spectra of reaction centers (2.0 μM) in 1.0 ml buffer (0.025% LDAO, 10 mM Tris-Cl, pH 8) were taken before and after addition of a stoichiometric amount of quinone (6.5 μl of 320 μM UQ-50 in 10% LDAO). The reference compartment also contained a 2.0 μM reaction center solution in buffer. Also added was an equal amount of detergent solution with no quinone to eliminate differences due to concentration changes or detergent effects. The spectra before and after quinone addition were stored on a Nicolet 1180 computer and subtracted to give the spectra shown above. Each spectrum represents the average of four scans. The maximum absorbance in the sample was 0.6. The gains were adjusted so that the spectral resolution was always better than 1.2 nm. The spectrum of UQ-50 in LDAO was obtained by adding the same amount of UQ-50 to the buffer solution.

450 nm (*27*, *40*, *47*, *48*). This absorption peak is characteristic of the ubisemiquinone anion radical which, in methanol, has a peak near 445 nm (*49*, *50*). The similarity between the ubisemiquinone spectrum in reaction centers and *in vitro* provides another argument against quinone ligation to Fe^{2+}, since direct coordination would be expected to cause a larger change in the semiquinone spectrum. However, the UV difference spectra of the quinones in reaction centers are shifted to longer wavelengths (*47*, *48*). We reinvestigated these shifts by taking the difference spectrum of quinone-depleted reaction centers before and after addition of quinone. The spectrum of a stoichiometric amount of UQ-50 added to reaction centers is shown in Fig. 10, along with the spectrum of the same amount of UQ-50 added to buffer.

The spectrum of the quinone in the reaction center shows a long wavelength shift to 285 nm from ~275 nm in buffer. In addition, a sug-

TABLE II

Absorbance Maxima for UQ-50 in Various Solvents

Solvent	λ_{max} (nm)
Cyclohexane	272 ± 1
t-Butanol	274
Isopropanol	275
Ethanol	275
Acetic acid	275
1% LDAO in H_2O	276
Q_I in RC	285

gestion of a shoulder appears in the 300 nm region. Spectra of Q_{II} in the reaction center could not be easily obtained since an excess of quinone is required to saturate the site. However, preliminary results indicate that the Q_{II} spectrum shows a similar shift. When Vitamin K_1, a menaquinone, was added to reaction centers, small shifts to longer wavelengths were observed in all peaks. In addition, a marked shoulder appeared around 288 nm. To explain these spectral changes, measurements were made on UQ-50 dissolved in various solvents (Table II). The quinone absorption peak shifted to longer wavelengths as the polarity of the solvent was increased; this is indicative of a $\pi \rightarrow \pi^*$ transition (*51*). However, in none of the solvents was the shift nearly as large as that observed in reaction centers. This rules out a simple solvent effect. One possible explanation for the large shift is an interaction of the quinone with either (BPh), Fe^{2+}, or aromatic amino acid residues in the protein. Another possibility is the presence of large electric fields, perhaps resulting from a net charge or fixed dipoles, that stabilizes the polar excited state.

ENDOR Another spectroscopic probe of the quinone in the reaction center is electron nuclear double resonance (ENDOR) spectroscopy. ENDOR gives information about the spin density distribution of paramagnetic molecules. ENDOR spectra were obtained of ubisemiquinone in the Q_I site of reaction centers after removal of the Fe^{2+} (*52*). These spectra are similar but not identical to ENDOR spectra of ubisemiquinone obtained *in vitro* (*53*). It is not yet known whether these differences are due to specific features of the quinone binding site in the reaction center. Theoretical studies of the spin densities should help to provide an explanation (*54*).

SUMMARY AND DISCUSSION

We have briefly summarized some of the spectroscopic and structural properties of the two quinones bound to bacterial reaction centers. The primary quinone Q_I is tightly bound and is close to the M subunit as well as to the (BPh) that serves as its immediate electron donor. The distance between Q_I and (BPh), estimated from EPR measurements, is 7 to 10 Å. The secondary quinone Q_{II} is more weakly bound to the M subunit. Preliminary data suggests that the H subunit is also involved in providing an active binding site. Both Q_I and Q_{II}, as shown by EPR spectroscopy, are magnetically coupled to the Fe^{2+} and must, therefore, be in close proximity. However, magnetic susceptibility, EXAFS, Mossbauer, and optical absorption spectroscopy indicate that neither quinone is directly coordinated to the Fe^{2+}. One possible structure of the ferroquinone complex involves close association of both quinones with an aromatic ligand or ligands of Fe^{2+}, for example, tryosine or histidine residues. Such an association may explain the large wavelength shift observed in the UV absorption spectrum of both Q_I and Q_{II}. The unusual stability of the semiquinone state of Q_I, and to some extent Q_{II}, could arise from an aprotic environment which prevents protonation leading to two-electron reduction. Alternatively, the stabilization may be caused by the presence of fixed positive charges that may be provided by Fe^{2+}.

In conclusion, the bacterial reaction center provides a good example of a quinone-containing protein complex. Understanding the structure and function of quinone binding sites in reaction centers may lead to a better understanding of other quinone-protein complexes in biology.

ACKNOWLEDGMENTS

We would like to thank Chang-An Yu for providing samples of UQ-10 and UQ-0-decyl, Ed Abresch for preparing the reaction centers, Roger Isaacson for assistance in many of the measurements, and Gunars Valkirs for preparation and characterization of the antibodies. This work was supported by grants from the NSF (PCM 78-13699), and the NIH (GM 13191).

REFERENCES

1. Arnon, D. I., and Crane, F. L. (1965). *In* "Biochemistry of Quinones" (R. A. Morton, ed.), pp. 433–459. Academic Press, New York.
2. Loach, P. A. (1976). *Prog. Bioorg. Chem.* **4,** 89–192.

3. Feher, G., and Okamura, M. Y. (1978). *In* "The Photosynthetic Bacteria" (R. K. Clayton and W. R. Sistrom, eds.), pp. 349–386. Plenum, New York.
4. Dutton, P. L., Prince, R. C., and Tiede, P. M. (1978). *Photochem. Photobiol.* **28,** 939–949.
5. Okamura, M. Y., Feher, G., and Nelson, N. (1982). *In* Photosynthesis, Energy Conversion by Plants and Bacteria" (Govindjee, ed.). Academic Press, New York. To be published.
6. Parson, W. W. (1978). *In* "The Photosynthetic Bacteria" (R. K. Clayton and W. R. Sistrom, eds.), pp. 455–470. Plenum, New York.
7. Bolton, J. R. (1978). *In* "The Photosynthetic Bacteria" (R. K. Clayton and W. R. Sistrom, eds.), pp. 419–430. Plenum, New York.
8. Wraight, C. A. (1979). *Photochem. Photobiol.* **30,** 767–776.
9. Blankenship, R. E., and Parson, W. W. (1979). *Annu. Rev. Biochem.* **47,** 635–653.
10. Parson, W. W., and Ke, B. (1981). *In* "Integrated Approach to Plant and Bacterial Photosynthesis" (Govindjee, ed.). Academic Press, New York.
11. Cogdell, R. J., Brune, D. C., and Clayton, R. K. (1974). *FEBS Lett.* **45,** 344–347.
12. Okamura, M. Y., Isaacson, R. A., and Feher, G. (1975). *Proc. Natl. Acad. Sci. U.S.A.* **72,** 3491–3495.
13. Clayton, R. K., and Yau, H. F. (1972). *Biophys. J.* **12,** 867–881.
14. Blankenship, R. E., and Parson, W. W. (1979). *Biochim. Biophys. Acta* **545,** 429–444.
15. Parson, W. W. (1968). *Biochim. Biophys. Acta* **153,** 248–259.
16. Clayton, R. K., Fleming, H., and Szuts, E. Z. (1972). *Biophys. J.* **12,** 46–63.
17. Marinetti, T. D., Okamura, M. Y., and Feher, G. (1979). *Biochemistry* **18,** 3126–3133.
18. Valkirs, G. and Feher, G. (1981). *Biophys. J.* **33,** 18a.
19. Debus, R. J., Valkirs, G., Okamura, M. Y., and Feher, G. To be published.
20. Okamura, M. Y., Steiner, L. A., and Feher, G. (1974). *Biochemistry* **13,** 1394–1403.
21. Debus, R. J., Okamura, M. Y., and Feher, G. (1981). *Biophys. J.* **33,** 19a.
22. McElroy, J. D., Feher, G., and Mauzerall, D. C. (1970). *Biophys. Soc. Abstr.* **10,** 204.
23. Feher, G. (1971). *Photochem. Photobiol.* **14,** 373–388.
24. Dutton, P. L., Leigh, J. S., and Reed, D. W. (1973). *Biochim. Biophys. Acta* **292,** 654–664.
25. Loach, P. A., and Hall, R. L. (1972). *Proc. Natl. Acad. Sci. U.S.A.* **69,** 786–790.
26. Feher, G., Okamura, M. Y., and McElroy, J. D. (1972). *Biochim. Biophys. Acta* **267,** 222–226.
27. Wraight, C. A. (1977). *Biochim. Biophys. Acta* **459,** 525–531.
28. Wraight, C. A. (1978). *FEBS Lett.* **93,** 283–288.
29. Okamura, M. Y., Isaacson, R. A., and Feher, G. (1978). *Biophys. J.* **21,** 8a.
30. Butler, W. F., Johnston, D. C., Shore, H. B., Fredkin, D. R., Okamura, M. Y., and Feher, G. (1980). *Biophys. J.* **32,** 967–992.
31. Kessel, S. L., Emberson, R. M., Debrunner, P. G., and Hendrickson, D. N. (1980). *Inorg. Chem.* **19,** 1170–1178.
32. Coffman, R. E., and Buettner, G. R. (1979). *J. Phys. Chem.* **83,** 2387–2392.
33. Boso, B., Debrunner, P., Okamura, M. Y., and Feher, G., (1981). *Biochim. Biophys. Acta* **638,** 173–177.
34. Eisenberger, P. M., Okamura, M. Y., and Feher, G. (1980). *Fed. Proc., Fed. Am. Soc. Exp. Biol.* **39,** 1802.
35. Bunker, G., Stern, E. A., Blankenship, R. E., and Parson, W. W., (1982). *Biophys J.*, **37,** 539–551.
36. Eisenberger, P. M., Okamura, M. Y., and Feher, G. (1982). *Biophys J.*, **37,** 523–538.

37. Parson, W. W., Clayton, R. K., and Cogdell, R. J. (1975). *Biochim. Biophys. Acta* **387,** 265–278.
38. Fajer, J., Brune, D. C., Davis, M. S., Forman, A., and Spaulding, L. D. (1975). *Proc. Natl. Acad. Sci. U.S.A.* **72,** 4956–4960.
39. Loach, P. A. (1966). *Biochemistry* **5,** 592–600.
40. Clayton, R. K., and Straley, S. C. (1972). *Biophys. J.* **12,** 1221–1234.
41. Vermeglio, A., and Clayton, R. K. (1977). *Biochim. Biophys. Acta* **461,** 159–165.
42. Tiede, D. M., Prince, R. C., and Dutton, P. L. (1976). *Biochim. Biophys. Acta* **449,** 447–467.
43. Okamura, M. Y., Isaacson, R. A., and Feher, G. (1979). *Biochim. Biophys. Acta* **546,** 394–417.
44. Hopfield, J. J. (1977). *In* "Electrical Phenomena at the Biological Membrane Level" (E. Roux, ed.), pp. 471–492. Elsevier, Amsterdam.
45. Peters, K., Avouris, P., and Rentzepis, P. M. (1978). *Biophys. J.* **23,** 207–217.
46. Gast, P., and Hoff, A. J. (1979). *Biochim. Biophys. Acta* **548,** 520–535.
47. Slooten, L. (1972). *Biochim. Biophys. Acta* **276,** 208–218.
48. Vermeglio, A. (1977). *Biochim. Biophys. Acta* **459,** 516–524.
49. Land, E. J., Simic, M., and Swallow, A. J. (1971). *Biochim. Biophys. Acta* **226,** 239–240.
50. Bensasson, R., and Land, E. J. (1973). *Biochim. Biophys. Acta* **325,** 175–181.
51. Morton, R. A. (1965). *In* "Biochemistry of Quinones" (R. A. Morton, ed.), pp. 23–66. Academic Press, New York.
52. Okamura, M. Y., Debus, R. J., Isaacson, R. A., Feher, G. (1980). *Fed. Proc., Fed. Am. Soc. Exp. Biol.* **39,** 1802.
53. Das, M. R., Conner, H. D., Leniart, D. S., and Freed, J. H. (1970). *J. Am. Chem. Soc.* **92,** 2258.
54. Coker, A., Mishra, K. C., and Das, T. P. (1980). *Fed. Proc., Fed. Am. Soc. Exp. Biol.* **39,** 1802.
55. McElroy, J. D., Mauzerall, D. C., and Feher, G. (1974). *Biochim. Biophys. Acta* **333,** 261–277.